PCCP

COMMUNICATION

View Article Online
View Journal

Cite this: DOI: 10.1039/c5cp03059e

Received 27th May 2015,
Accepted 2nd August 2015

DOI: 10.1039/c5cp03059e

www.rsc.org/pccp

The time scale of the quaternary structural changes in hemoglobin revealed using the transient grating technique†

Cheolhee Yang,[ab] Jungkweon Choi[b] and Hyotcherl Ihee*[ab]

The quaternary structural transition between the R and T states of human hemoglobin was investigated using the transient grating technique. The results presented herein reveal that the quaternary structural change accompanied by the R–T transition occurs within a few microseconds.

Many proteins undergo conformational changes that are directly linked with their functions *in vivo*. Human hemoglobin (Hb), which carries oxygen in red blood cells, is a textbook example of such a protein. Hb has a tetrameric structure comprising four subunits (α_1, α_2, β_1, and β_2), each of which contains a heme group capable of binding ligands such as O_2 and CO. The binding of ligands to Hb is a cooperative process, leading to a structural change between the following two states of Hb: relaxed (R) and tense (T) states. The high-affinity R state is stabilized by binding of ligands, while the stable low-affinity T state is formed upon dissociation of ligands. Thus, dissociation of ligands from Hb induces the R–T transition involving a quaternary structural change in which one αβ dimer rotates with respect to the other.

The R–T transition in Hb has been experimentally[1–21] and theoretically[22–28] investigated *via* the photodissociation reaction of ligated Hb, *e.g.*, carbonmonoxy Hb (HbCO). A variety of time-resolved techniques, such as transient absorption (TA) spectroscopy,[1–4] time-resolved UV resonance Raman spectroscopy (TR-UVRR),[4,11,12,16,17] time-resolved wide-angle X-ray scattering (TR-WAXS),[5,6,15] time-resolved IR spectroscopy,[13,14] *etc.*, have been used to investigate the photodissociation of HbCO. Accordingly, many kinetic components, summarized in Fig. 1, have been observed. As shown in Fig. 1, the time constants from various studies on the dynamics of the R–T transition are scattered over a wide time range from hundreds of nanoseconds to tens of microseconds. One of the key questions is which kinetics within this broad time window is primarily responsible for the quaternary structural change associated with the R–T transition. To address this question, herein we used the TG technique, which is a useful tool for sensitively probing the global structural change of a protein by monitoring changes in the diffusion coefficient.[29–40]

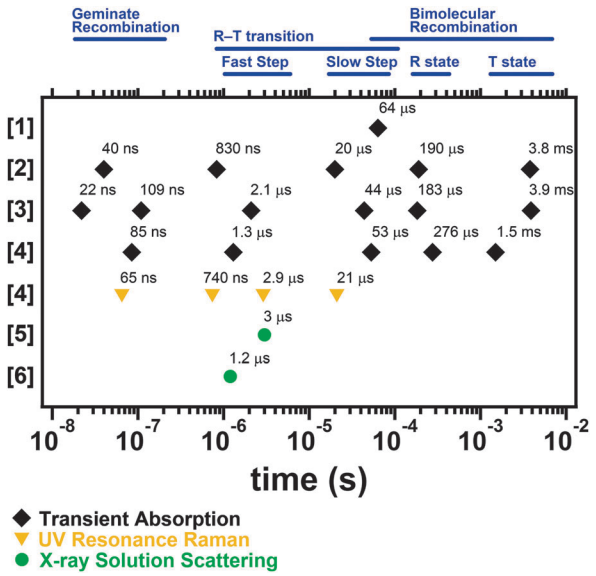

Fig. 1 Comparison of the kinetics of Hb induced by photodissociation of the CO ligand obtained using various time-resolved techniques. The numbers on the left side indicate the reference numbers. The processes related to the observed time constants are shown on the top of the figure (blue line).

Before using the TG technique, for comparison with previous studies, we first measured the TA spectra of HbCO in 100 mM sodium phosphate buffer (pH 7.0) and observed four relaxation times of 1.2 μs, 48 μs, 310 μs, and 6.0 ms (Fig. S1, ESI†). These time constants agree with those reported in previous TA studies (Fig. 1).[1–4] The comparison of the relaxation

[a] Department of Chemistry, KAIST, Daejeon 305-701, Republic of Korea. E-mail: hyotcherl.ihee@kaist.ac.kr; Fax: +82-42-350-2810; Tel: +82-42-350-2884
[b] Center for Nanomaterials and Chemical Reactions, Institute for Basic Science (IBS), Daejeon 305-701, Republic of Korea

† Electronic supplementary information (ESI) available: Transient absorption spectra of HbCO and singular value decomposition results of the TA spectra, details of experimental methods and theoretical background of the TG experiment. See DOI: 10.1039/c5cp03059e

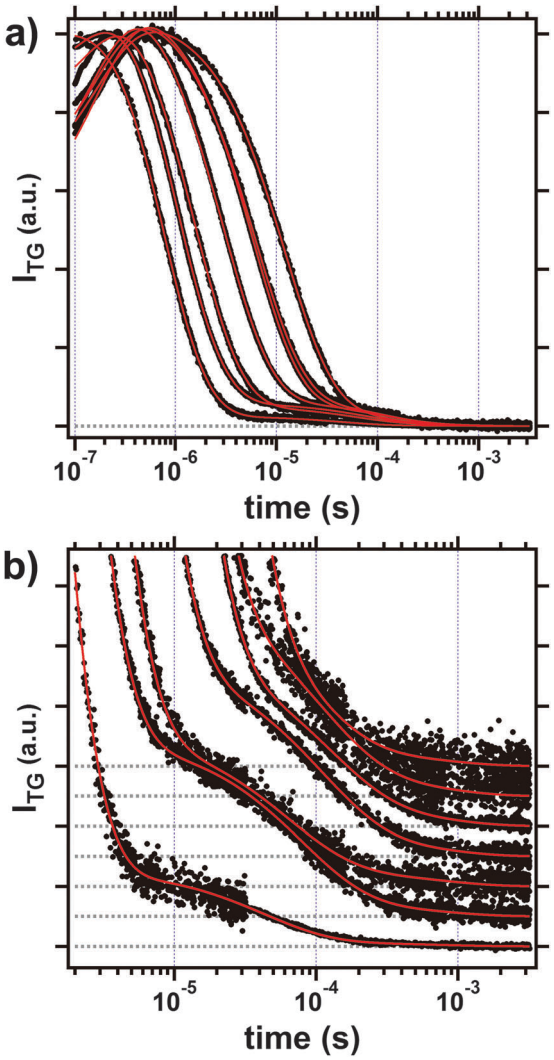

Fig. 2 (a) Transient grating (TG) signals of 300 μM HbCO in 100 mM phosphate buffer (pH 7) excited at 532 nm at various q^2 values (from right to left, q^2 = 0.35, 0.70, 0.76, 1.44, 2.79, 4.16, and 5.27 × 10^{12} m^{-2}). The experimental data (black) at various q^2 values were fitted *via* global fitting analysis in which a square of a sum of exponentials sharing common time constants is used to represent each theoretical curve (red), resulting in theoretical curves that are in satisfactory agreement with the experimental data. (b) Enlarged view of the TG signals after 1 μs.

times with previous TA results shown in Fig. 1 indicates that the relaxation times at 1.2 and 48 μs are related to the R–T transition while those at 310 μs and 6.0 ms were assigned to the pseudo-first order time constants for the bimolecular recombination of CO to the R and T states of Hb, respectively.

Fig. 2 shows the TG signals after photoexcitation of HbCO in 100 mM sodium phosphate buffer (pH 7) at various grating wavenumbers (q^2). All TG signals quickly increase within the excitation pulse width, followed by a weak increase at a sub-μs time scale. The TG signals then show strong and weak decay features at a few μs and several hundred μs, respectively.

Because the absorbance change of the sample is undetectable at the probe wavelength of 780 nm, the intensity of the TG signal (I_{TG}) is proportional to the square of the refractive index change (δn) only. Thus, I_{TG} can be expressed by

$$I_{TG}(t) = \alpha[\delta n(t)]^2, \quad (1)$$

where α is a constant determined by the experimental conditions. δn is attributed to the thermal effect (thermal grating, δn_{th}) and the chemical species involved in the photoreaction (species grating, δn_{spe}). From a quantitative analysis of all the TG signals, we determined that all the TG signals observed at various q^2 values can be well reproduced by the square of the sum of five exponential functions as follows:

$$I_{TG}(t) = \alpha[\delta n_1 \exp(-k_1 t) + \delta n_2 \exp(-k_2 t) + \delta n_3 \exp(-k_3 t) + \delta n_4 \exp(-k_4 t) + \delta n_5 \exp(-k_5 t)]^2, \quad (2)$$

where δn_i and k_i are the refractive index changes and rate constants of the ith exponential relaxation, respectively.

The three rate constants, k_1, k_3, and k_5, show constant values regardless of the q^2 value, while the values of k_2 and k_4 exhibit q^2-dependence. The thermal grating signal originates from a temperature change in the medium caused by the thermal relaxation from the excited states and enthalpy change during the reaction. The decay rate of the thermal grating (k_{th}) can be easily determined from the thermal diffusivity (D_{th}) and q^2 values, as follows: $k_{th} = D_{th} \times q^2$. Considering the thermal diffusivity under the experimental conditions, the decay feature with the rate constant k_2 was assigned to the thermal grating signal. The slower dynamics of k_4, which depends on the q^2 value, was attributed to the diffusion processes of chemical species such as HbCO, Hb or CO. Because the rate of the diffusion process is expressed as the product of the diffusion coefficient (D) with q^2, the diffusion coefficient of a chemical species can be calculated from a plot of the rate constants against the q^2 values. As shown in Fig. 3, the k_4 values show a linear relationship with the q^2 values. From the slope of the plot, D was calculated to be 1.3 ± 0.1 × 10^{-9} m^2 s^{-1}. This value is close to the diffusion coefficient of CO that was reported previously (1.46–3.1 × 10^{-9} m^2 s^{-1}),[38,40,41] indicating that the q^2-dependence of k_4 is due to diffusion of the CO ligand released

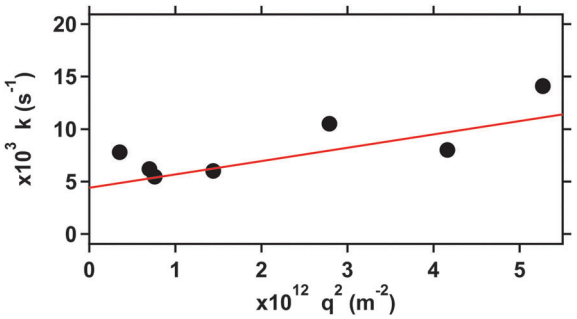

Fig. 3 Plot of rate constant, k_4 (black), of the TG signals *versus* q^2. From the slope of the plot (red), a diffusion coefficient (D) of 1.3 ± 0.1 × 10^{-9} m^2 s^{-1} was determined. This value is consistent with the previously reported diffusion coefficient of CO (1.46–3.1 × 10^{-9} m^2 s^{-1}). Moreover, the intercept of the plot of 4.4 ± 0.2 × 10^3 s^{-1} (230 ± 10 μs) was determined to be the rate constant.

by photodissociation of HbCO. Furthermore, the intercept of the plot, which was $4.4 \pm 0.2 \times 10^3$ s^{-1} (230 ± 10 μs), is close to the time constant corresponding to the bimolecular recombination of the CO ligand and R-state Hb (Fig. 1). Therefore, the diffusion of the CO ligand observed herein is due to recombination of the CO ligand and Hb in the R state ($Hb_R + CO \rightarrow HbCO$).

Even though the TG technique is very sensitive to changes of the diffusion coefficient of a protein, no diffusion of the protein species was observed in this study. In TG experiments, the species grating intensity is the difference between δn due to the reactant (δn_R) and product (δn_P). The sign of δn_P is positive, while the sign of δn_R is negative because the phase of the spatial concentration modulation of the product is shifted 180° from that of the reactant. In the photodissociation reaction of HbCO, the product is CO and Hb, and the reactant is HbCO. Since the molecular sizes of Hb and HbCO are very similar, the diffusion coefficients of the two species are similar ($D_{Hb} \approx D_{HbCO}$). Considering the $D_{Hb} \approx D_{HbCO}$ condition, the difference between the refractive index changes of Hb and HbCO, *i.e.*, the difference between δn_R and δn_P, can be expressed as eqn (S6) (ESI†). Consequently, the absence of the diffusion process of the protein species is probably because δn_R and δn_P have similar values ($\delta n_R \approx \delta n_P$), which cause eqn (S6) (ESI†) to be irrelevant.

On the other hand, the q^2-independence of k_1, k_3, and k_5 indicates that the dynamics corresponding to each rate constant are the reaction kinetics that occur subsequent to the photodissociation of the CO ligand rather than diffusion of the chemical species. The relaxation times that correspond with k_1, k_3, and k_5 were determined to be $6.4 \pm 0.1 \times 10^6$ s^{-1} (160 ± 3 ns), $5.9 \pm 0.3 \times 10^5$ s^{-1} (1.7 ± 0.1 μs), and 710 ± 50 s^{-1} (1.4 ± 0.1 ms), respectively. By comparing the relaxation times from the TG signals with the kinetics reported in previous studies (Fig. 1), we assign the 160 ns kinetics to geminate the recombination of the photodissociated CO ligand, while we assign the 1.4 ms kinetics to bimolecular recombination of the CO ligand and Hb in the T state.

Finally, we need to discuss the origin of the 1.7 μs kinetics observed in the TG signal. It is known that the TG signal is very sensitive to the volume change induced by the conformational change of a protein.[29–40] Theoretically, the species grating (δn_{spe}) arises from the change in the absorption spectrum (population grating, δn_p) and the change in the molecular volume (volume grating, δn_v), as follows: $\delta n_{spe} = \delta n_p + \delta n_v$. The volume grating is expressed by

$$\delta n_v = V\left(\frac{dn}{dV}\right)\Delta V \Delta N, \quad (3)$$

where (dn/dV) is the refractive index change caused by the molecular volume change, ΔV is the volume change during the reaction, and ΔN is the number of reacting molecules in a unit volume. Since the absorbance change is undetectable at the wavelength of the probe beam used during the photoreaction of Hb, the contribution of δn_p to the measured TG signals should be negligible. Considering the term ΔV in eqn (3), the dynamics at 1.7 μs should be due to the large volume change that accompanies the conformational change of Hb. Indeed, the quaternary structural change that occurs upon the R–T transition should induce a large volume change. Therefore, based on the principles of the TG measurements, we suggest that the dynamics at 1.7 μs observed in the TG experiments is due to the quaternary structural change accompanied by the R–T transition, which leads to a large volume change. On the other hand, the TG signal does not show the dynamics of tens of μs observed in TA and UVRR studies.[1–4,11,12] The absence of the dynamics of tens of μs in TG results implies that the volume change induced by the dynamics at tens of μs is small compared to that induced by the dynamics at 1.7 μs. One cannot rule out the possibility that the observed dynamics of the TG signal at 1.7 μs is due to the transition between the tertiary forms within a given quaternary state. The studies on the kinetics of Hb by using sol–gel encapsulation[19,21] showed that Hb trapped in gel matrices has the high- and low-affinity states, suggesting that there are tertiary forms having different ligand affinities in a given quaternary state. In addition, a theoretical study of R–T transition supported the results of the encapsulation studies by suggesting the tertiary and quaternary structural changes in the R–T transition can be uncoupled.[22] However, the volume change of the quaternary structural change should be larger than that of the tertiary structural change, and for this reason we suggest that the dynamics at 1.7 μs is due to the quaternary structural change of the R–T transition rather than the tertiary structural change within a given quaternary state.

Our interpretation of the dynamics at 1.7 μs is in contrast to the results reported by previous studies using the TA technique. The studies using TA spectroscopy in the 1970s and 1980s suggested that the decaying kinetics at several tens of μs is due to the R–T transition because the TA spectrum corresponding to that time scale is very similar to the difference spectrum between the absorption spectra of the R and T states.[1,2] Meanwhile, the faster relaxation observed within the sub- μs to a few μs time range was assigned to the tertiary structural change.[2] Later, other studies using TA spectroscopy, singular value decomposition (SVD) and kinetic modelling suggested that the fast relaxation occurring within a few μs could also be related to the R–T transition although the slow dynamics at the tens of μs time scale was interpreted as the major quaternary structural change due to the R–T transition.[3,8] In contrast to the results obtained by TA experiments, in the studies using time-resolved optical rotatory dispersion (TRORD)[9] and time-resolved circular dispersion (TRCD),[10] the spectral change occurring within ~1 μs time scale was observed and interpreted as the movement of several amino acid residues located near the dimer–dimer interface associated with the R–T transition. Similarly, in a study using time-resolved magnetic circular dichroism (TRMCD),[18] a shift in the tryptophan MCD band with a time constant of 2 μs was observed and interpreted as evidence for the appearance of a T-state hydrogen bond (Trp β37-Asp α94). On the other hand, in the studies using TR-UVRR spectroscopy, the biphasic structural changes of the hydrogen bonds in the dimer–dimer interface, which are known as the hinge contact and switch contact formations, respectively, were observed and assigned to the R–T transition.[4,11,12,20] According to this assignment, the hinge

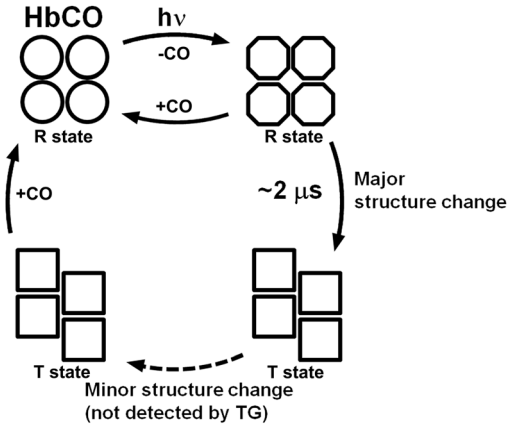

Fig. 4 Kinetic model that is compatible with the TG signals. The process represented by a dotted arrow was detected using TA spectroscopy but not the TG technique.

contact was made within a few μs and then the switch contact was formed within tens of μs. Recently, the studies using TR-WAXS technique, which can monitor the conformational changes of various biomolecules occurring in the solution phase,[5,6,15,42–54] revealed that the significant scattering signal change was observed mainly at a few μs time scale and assigned to the R–T transition.[5,6,15] Moreover, a theoretical study using the conjugate peak refinement (CPR) method exhibited that the tertiary and quaternary transitions from T to R states were not coupled with each other and that the quaternary structural changes occurred in two steps, *i.e.*, Q1 and Q2.[22] In the direction from R to T, the faster Q2 step induces a larger structural change than the slower Q1 step. These theoretical and experimental results are consistent with our results presented herein. Therefore, we conclude that the dynamics at 1.7 μs observed in the TG experiments is due to the quaternary structural change accompanied by the R–T transition, which leads to a large volume change.

In summary, we studied the quaternary structural change of Hb using the TG technique. The data presented herein demonstrate that the dynamics at ~2 μs observed in the TG experiment is due to the volume change caused by the quaternary structural change of Hb. This indicates that the dynamics at ~2 μs corresponds to the fast step of the R–T transition, leading to a major quaternary structural change of Hb as shown in Fig. 4.

Acknowledgements

This work was supported by IBS-R004-G2.

Notes and references

1 C. A. Sawicki and Q. H. Gibson, *J. Biol. Chem.*, 1976, **251**, 1533–1542.
2 J. Hofrichter, J. H. Sommer, E. R. Henry and W. A. Eaton, *Proc. Natl. Acad. Sci. U. S. A.*, 1983, **80**, 2235–2239.
3 R. A. Goldbeck, S. J. Paquette and D. S. Kliger, *Biophys. J.*, 2001, **81**, 2919–2934.
4 G. Balakrishnan, M. A. Case, A. Pevsner, X. J. Zhao, C. Tengroth, G. L. McLendon and T. G. Spiro, *J. Mol. Biol.*, 2004, **340**, 843–856.
5 M. Cammarata, M. Levantino, F. Schotte, P. A. Anfinrud, F. Ewald, J. Choi, A. Cupane, M. Wulff and H. Ihee, *Nat. Methods*, 2008, **5**, 881–886.
6 M. Cammarata, M. Levantino, M. Wulff and A. Cupane, *J. Mol. Biol.*, 2010, **400**, 951–962.
7 V. Jayaraman, K. R. Rodgers, I. Mukerji and T. G. Spiro, *Science*, 1995, **269**, 1843–1848.
8 R. A. Goldbeck, S. J. Paquette, S. C. Bjorling and D. S. Kliger, *Biochemistry*, 1996, **35**, 8628–8639.
9 D. B. Shapiro, R. A. Goldbeck, D. P. Che, R. M. Esquerra, S. J. Paquette and D. S. Kliger, *Biophys. J.*, 1995, **68**, 326–334.
10 S. C. Bjorling, R. A. Goldbeck, S. J. Paquette, S. J. Milder and D. S. Kliger, *Biochemistry*, 1996, **35**, 8619–8627.
11 E. M. Jones, E. Monza, G. Balakrishnan, G. C. Blouin, P. J. Mak, Q. H. Zhu, J. R. Kincaid, V. Guallar and T. G. Spiro, *J. Am. Chem. Soc.*, 2014, **136**, 10325–10339.
12 G. Balakrishnan, C. H. Tsai, Q. Wu, M. A. Case, A. Pevsner, G. L. McLendon, C. Ho and T. G. Spiro, *J. Mol. Biol.*, 2004, **340**, 857–868.
13 S. Kim, J. Heo and M. Lim, *J. Am. Chem. Soc.*, 2006, **128**, 2810–2811.
14 S. Kim and M. Lim, *J. Am. Chem. Soc.*, 2005, **127**, 5786–5787.
15 M. Levantino, A. Spilotros, M. Cammarata, G. Schiro, C. Ardiccioni, B. Vallone, M. Brunori and A. Cupane, *Proc. Natl. Acad. Sci. U. S. A.*, 2012, **109**, 14894–14899.
16 Y. Mizutani and M. Nagai, *Chem. Phys.*, 2012, **396**, 45–52.
17 K. Yamada, H. Ishikawa, M. Mizuno, N. Shibayama and Y. Mizutani, *J. Phys. Chem. B*, 2013, **117**, 12461–12468.
18 R. A. Goldbeck, R. M. Esquerra and D. S. Kliger, *J. Am. Chem. Soc.*, 2002, **124**, 7646–7647.
19 U. Samuni, L. Juszczak, D. Dantsker, I. Khan, A. J. Friedman, J. Perez-Gonzalez-De-Apodaca, S. Bruno, H. L. Hui, J. E. Colby, E. Karasik, L. D. Kwiatkowski, A. Mozzarelli, R. Noble and J. M. Friedman, *Biochemistry*, 2003, **42**, 8272–8288.
20 T. G. Spiro and G. Balakrishnan, *J. Mol. Biol.*, 2010, **400**, 949–950.
21 C. Viappiani, S. Bettati, S. Bruno, L. Ronda, S. Abbruzzetti, A. Mozzarelli and W. A. Eaton, *Proc. Natl. Acad. Sci. U. S. A.*, 2004, **101**, 14414–14419.
22 S. Fischer, K. W. Olsen, K. Nam and M. Karplus, *Proc. Natl. Acad. Sci. U. S. A.*, 2011, **108**, 5608–5613.
23 W. A. Eaton, E. R. Henry and J. Hofrichter, *Proc. Natl. Acad. Sci. U. S. A.*, 1991, **88**, 4472–4475.
24 L. Mouawad and D. Perahia, *J. Mol. Biol.*, 1996, **258**, 393–410.
25 L. Mouawad, D. Perahia, C. H. Robert and C. Guilbert, *Biophys. J.*, 2002, **82**, 3224–3245.
26 Y. Seno, *J. Comput. Chem.*, 2006, **27**, 701–710.
27 M. Laberge and T. Yonetani, *Biophys. J.*, 2008, **94**, 2737–2751.
28 J. S. Hub, M. B. Kubitzki and B. L. de Groot, *PLoS Comput. Biol.*, 2010, **6**, e1000774.
29 S. Nishida, T. Nada and M. Terazima, *Biophys. J.*, 2005, **89**, 2004–2010.

30 J. Choi, Y. O. Jung, J. H. Lee, C. Yang, B. Kim and H. Ihee, *ChemPhysChem*, 2008, **9**, 2708–2714.
31 J. Choi, C. Yang, J. Kim and H. Ihee, *J. Phys. Chem. B*, 2011, **115**, 3127–3135.
32 Y. Nakasone, T. Ono, A. Ishii, S. Masuda and M. Terazima, *Biochemistry*, 2010, **49**, 2288–2296.
33 K. Tanaka, Y. Nakasone, K. Okajima, M. Ikeuchi, S. Tokutomi and M. Terazima, *FEBS Lett.*, 2011, **585**, 786–790.
34 Y. Nakasone, Y. Kawaguchi, S. G. Kong, M. Wada and M. Terazima, *J. Phys. Chem. B*, 2014, **118**, 14314–14325.
35 Y. Nakasone, K. Zikihara, S. Tokutomi and M. Terazima, *Photochem. Photobiol. Sci.*, 2013, **12**, 1171–1179.
36 K. Takeda, Y. Nakasone, K. Zikihara, S. Tokutomi and M. Terazima, *J. Phys. Chem. B*, 2013, **117**, 15606–15613.
37 Y. Hoshihara, Y. Lmamoto, M. Kataoka, F. Tokunaga and M. Terazima, *Biophys. J.*, 2008, **94**, 2187–2193.
38 M. Sakakura, S. Yamaguchi, N. Hirota and M. Terazima, *J. Am. Chem. Soc.*, 2001, **123**, 4286–4294.
39 Y. Nishihara, M. Sakakura, Y. Kimura and M. Terazima, *J. Am. Chem. Soc.*, 2004, **126**, 11877–11888.
40 J. Choi, S. Muniyappan, J. T. Wallis, W. E. Royer and H. Ihee, *ChemPhysChem*, 2010, **11**, 109–114.
41 T. Hara, N. Hirota and M. Terazima, *J. Phys. Chem.*, 1996, **100**, 10194–10200.
42 S. Ahn, K. H. Kim, Y. Kim, J. Kim and H. Ihee, *J. Phys. Chem. B*, 2009, **113**, 13131–13133.
43 P. L. Ramachandran, J. E. Lovett, P. J. Carl, M. Cammarata, J. H. Lee, Y. O. Jung, H. Ihee, C. R. Timmel and J. J. van Thor, *J. Am. Chem. Soc.*, 2011, **133**, 9395–9404.
44 K. H. Kim, K. Y. Oang, J. Kim, J. H. Lee, Y. Kim and H. Ihee, *Chem. Commun.*, 2011, **47**, 289–291.
45 J. Kim, K. H. Kim, J. G. Kim, T. W. Kim, Y. Kim and H. Ihee, *J. Phys. Chem. Lett.*, 2011, **2**, 350–356.
46 K. H. Kim, S. Muniyappan, K. Y. Oang, J. G. Kim, S. Nozawa, T. Sato, S. Y. Koshihara, R. Henning, I. Kosheleva, H. Ki, Y. Kim, T. W. Kim, J. Kim, S. Adachi and H. Ihee, *J. Am. Chem. Soc.*, 2012, **134**, 7001–7008.
47 T. W. Kim, J. H. Lee, J. Choi, K. H. Kim, L. J. van Wilderen, L. Guerin, Y. Kim, Y. O. Jung, C. Yang, J. Kim, M. Wulff, J. J. van Thor and H. Ihee, *J. Am. Chem. Soc.*, 2012, **134**, 3145–3153.
48 K. Y. Oang, J. G. Kim, C. Yang, T. W. Kim, Y. Kim, K. H. Kim, J. Kim and H. Ihee, *J. Phys. Chem. Lett.*, 2014, **5**, 804–808.
49 K. Y. Oang, K. H. Kim, J. Jo, Y. M. Kim, J. G. Kim, T. W. Kim, S. Jun, J. Kim and H. Ihee, *Chem. Phys.*, 2014, **442**, 137–142.
50 H. S. Cho, F. Schotte, N. Dashdorj, J. Kyndt and P. A. Anfinrud, *J. Phys. Chem. B*, 2013, **117**, 15825–15832.
51 M. Andersson, E. Malmerberg, S. Westenhoff, G. Katona, M. Cammarata, A. B. Wohri, L. C. Johansson, F. Ewald, M. Eklund, M. Wulff, J. Davidsson and R. Neutze, *Structure*, 2009, **17**, 1265–1275.
52 E. Malmerberg, Z. Omran, J. S. Hub, X. W. Li, G. Katona, S. Westenhoff, L. C. Johansson, M. Andersson, M. Cammarata, M. Wulff, D. van der Spoel, J. Davidsson, A. Specht and R. Neutze, *Biophys. J.*, 2011, **101**, 1345–1353.
53 H. Ihee, *Acc. Chem. Res.*, 2009, **42**, 356–366.
54 E. Malmerberg, P. H. M. Bovee-Geurts, G. Katona, X. Deupi, D. Arnlund, C. Wickstrand, L. C. Johansson, S. Westenhoff, E. Nazarenko, G. F. X. Schertler, A. Menzel, W. J. de Grip and R. Neutze, *Sci. Signaling*, 2015, **8**, ra26.